

[Article]

www.whxb.pku.edu.cn

相对速率常数法测定几种还原态硫化物与·OH 反应速率常数

汪海涛 张玉洁 牟玉静*

(中国科学院生态环境研究中心, 北京 100085)

摘要: 利用 180-L Teflon 气袋, 采用相对速率方法测定了 298 K, 1.013×10^5 Pa 条件下·OH 自由基与 6 种还原态硫化物在空气、氮气和氧气体系下的反应速率常数. 所得结果与文献值进行了比较, 并讨论了氧气对速率常数的影响.

关键词: 速率常数; ·OH; 还原态硫化物

中图分类号: O643

Rate Constants for Reactions of ·OH with Several Reduced Sulfur Compounds Determined by Relative Rate Constant Method

WANG Hai-Tao ZHANG Yu-Jie MU Yu-Jin*

(Research Center for Eco-Environmental Sciences, Chinese Academy of Sciences, Beijing 100085, P. R. China)

Abstract: The rate constants for the reactions between ·OH and six reduced sulfur compounds in air, N_2 , and O_2 were measured using relative rate constant method in a 180-L Teflon bag at 298 K and 1.013×10^5 Pa. These results were compared with previous published data and were discussed in terms of trends in different buffer gases.

Key Words: Rate constant; ·OH; Reduced sulfur compound

Reduced sulfur compounds (R_1-S-R_2) (R_1 or $R_2=H$ or alkyl) are known to enter the atmosphere mainly from energy-relative activities, such as microbes, volcano, animal waste, wood pulp-ing, sewage treatment, and some of man-made sources. Their importance with respect to the atmospheric environment is that they have previously proposed adverse effects associated with acid rain, human health, climate modification, and visibility reduction. For example, dimethyl sulfide (DMS, CH_3SCH_3) is a kind of trace reduced sulfur compounds released by enzymatic cleavage of dimethylsulfoniopropionate (DMSP)^[1], which is synthesized by ubiquitous phytoplankton, and presents at parts per trillion levels in the Earth's troposphere^[2]. Hydrogen sulfide (H_2S) is another kind of important reduced sulfur compound. Volcanoes are now believed to be the largest nonanthropogenic contribution of H_2S to the atmosphere. Estimates of source strength of DMS and H_2S are (24.45 ± 5.30) and (7.72 ± 0.25) Tg·a⁻¹, respectively^[3]. The majority of DMS and H_2S released into the

atmosphere is removed by chemical reaction with ·OH and formed SO_2 which can be further oxidized to SO_4^{2-} (non-sea-salt sulfate, $NSS-SO_4^{2-}$). While $NSS-SO_4^{2-}$ is thought as the majority of cloud condensation nuclei (CCN). The albedo of cloud is sensitive to CCN density and has an effect of cooling down the global climate^[4]. This is contrary to the greenhouse gases, such as CO_2 , CH_4 , N_2O , and CFCs, which are thought to cause "global warming".

In order to understand and evaluate the impact that oxygenated R_1-S-R_2 (in a few cases, such as R_1 and R_2 are different series of substituents) will have on the environment, their atmospheric fate has to be known. It now appears that oxidation of R_1-S-R_2 , initiated by reaction with ·OH, is the most important process in atmospheric chemistry compared to a less extent of NO_3 . The rates of reactions of these compounds with other oxide, such as O_3 , are too slow to compete the reactions with ·OH and NO_3 in the atmosphere^[5,6]. Some studies on the rate constant data for ·OH with R_1-S-R_2 reactions have been reported. Sometimes it is

Received: February 13, 2008; Revised: March 6, 2008; Published on Web: April 10, 2008.

English edition available online at www.sciencedirect.com

*Corresponding author. Email: yjmu@rcees.ac.cn; Tel: +8610-62849125.

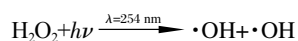
国家自然科学基金(20677067, 20577064)及国家重点基础研究发展规划项目(973) (2005CB422201)资助

found that rate constant (k) also depends on the pressure and the nature of the bath gas^[7]. Nevertheless, trends in parameters, such as the influence of O₂ partial pressure, are not well understood, and some complementary studies using smog chamber need have been simulated.

In the present work, we have conducted a number of relative rate measurements among hydrogen sulfide (H₂S), dimethyl sulfide (DMS, CH₃SCH₃), ethyl methyl sulfide (EMS, C₂H₅SCH₃), thioethanol (C₂H₅SH), *n*-butanethiol (*n*-C₄H₉SH, CH₃(CH₂)₃SH), and *iso*-butanethiol (*iso*-C₄H₉SH, (CH₃)₂CHCH₂SH) in nitrogen, air, and oxygen at (298.0±1.5) K. The advantage of this technique relative to absolute technique on resisting the interference of impurity provides a clearer picture of the rate constant trends among these reactants and offers some improvement in the reliability of the rate constant data. In addition, the relative rate constants derived in this work are compared with previously reported results and used to speculate on the residence time ($\tau_{R_1-S-R_2}$) of atmospheric reduced sulfur compounds.

1 Experimental

The apparatus and experimental procedures have been described elsewhere^[8] and will only be summarized here. Briefly, the experiments were carried out in an approximately 200-L heat-sealed Teflon bag, which was hung inside an iron box of 3 m³ with the internal walls covered with aluminum foil. A pair of electric fans was positioned on the opposite inner walls of the box to ensure that a uniform temperature can be maintained during reaction of the mixture. An electrothermal strip (2.6 cm in width and 600 cm in length, 600 W, BQ 16B, Shanghai Qianwu Wiring Factory, China) surrounds the inner chamber for heating. In all cases, the temperature variation in the chamber was maintained to be within ±1.5 K. A thermometer was used to monitor the temperature inside the chamber. The ·OH was generated through photolysis of H₂O₂ using four germicidal lamps (Philips, TUV 30 W with maximum output at 254 nm), which were set on the inner wall of chamber.



The ·OH generated reacts with the reduced sulfur compounds (S) and reference hydrocarbon compounds (R), with rate constants k_S and k_R , respectively:



Provided that reaction with ·OH is the only significant loss process for both reactant and reference compound, the decay of the reduced sulfur compounds (S) from [S]₀ at time $t=0$ to [S]_{*t*} at time t , and the simultaneous loss of the reference hydrocarbon compounds (R) from an initial concentration of [R]₀ to [R]_{*t*} at time t are given by Eq.(3).

$$\frac{k_S}{k_R} = \frac{\ln([S]_0/[S]_t)}{\ln([R]_0/[R]_t)} \quad (3)$$

Thus, a plot of $\ln([S]_0/[S]_t)$ vs $\ln([R]_0/[R]_t)$ should be a straight line passing through the origin and whose slope gives the ratio of rate constant k_S/k_R . The rate constant k_S could be derived from published values of k_R .

A mercury-free greaseless vacuum system was used for preparing gas mixtures. Pressure was measured with an MKS Baratron capacitance manometer ((0–1.33)×10⁴ Pa, MKS 270B). Measured amounts of the reagents were flushed from the quantified Pyrex bulbs into the Teflon reaction chamber by a stream of compressed air, which was purified by passing it through a charcoal column to remove hydrocarbon compounds. A mass flow meter (range: 0–5000 mL·min⁻¹, ShengYe Technology Company of Beijing, China) was used to control the flow rate. The two electrical fans were used to vibrate the Teflon bag gently in order to mix the reagents inside the bag. To obtain accurate constants of the studied reduced sulfur compounds using the relative method, the key work was to separate the studied reduced sulfur compounds from the reference compound, as well as, the studied reduced sulfur compounds and the reference compound from their degradation products during the course of photo-oxidation. Several tests were performed to check if there was any interference with analysis of DMS, EMS, or the reference before rate constant study. In all cases, neither the references nor the photo-oxidation products could infer through the analysis of the studied DMS, EMS, or the reference on our separation column used. A gas chromatograph (GC4410, East & West Analytical Instrument Inc., Beijing, China) equipped with a photoionization detector was used for the thiols quantitative analysis. Thiols in the reaction mixtures were separated on a 2 m×3 mm Teflon column packed with 30% Squalane on Chromosorb W (60–80 mesh) at a column temperature of 313 K. A gas chromatograph (GC-6AM, Shimadzu, Japan) equipped with a flame photometer detector (FPD) was used for H₂S, C₂H₅SH, and CH₃SCH₃ quantitative analysis. The H₂S, CH₃SCH₃, and SO₂ in the reaction mixtures were separated on a 3 m×4 mm glass column packed with 20% SE 30 on Chromosorb P (60–80 mesh). A gas chromatograph (GC-FID, HP5890, Agilent Technologies) equipped with flame ionization detector (FID) was used for other organic quantitative analysis. The references (propane and propene) in the reaction mixtures were separated on a 2 m×4 mm Teflon column packed with GDX 103 (60–80 mesh).

The following chemicals were used as received: propane, standard gas with mixing ratio of 3.97% (φ , volume fraction) in nitrogen; propene, standard gas with mixing ratio of 1.97% (φ) in nitrogen; H₂S, standard gas with mixing ratio of 0.229% (φ) in nitrogen. All these chemicals were products of National Research Center for Certified Reference Materials of China. DMS (Fluka, 98%), EMS, thioethanol, *n*-butanethiol, and *iso*-butanethiol (Merck, >95%) were further purified by repeat freeze, pump, and thaw cycles and fractional distillation before use; H₂O₂ (≥30%, Tianjin Oriental Chemical Plant, China); N₂ (>99.999%) and O₂ (>99.999%) were products of Beijing Haipu Gas Industry Company, China; Compressed air (Beijing Huayuan Gas Industry Company, China) was purified by passing it through silica gel, 3A molecular sieves, and active carbon before use.

It should be mentioned that the obvious losses of thiols and the reference compound by photolysis of the mixture of thiols, and the reference compound were observed under our experi-

Table 1 Summary of kinetics data for reaction of $\cdot\text{OH}$ with $\text{R}_1\text{—S—R}_2$

Reduced sulfur compound	Reference	Rate constants for $\cdot\text{OH}$ in different atmospheres ($\text{cm}^3 \cdot \text{molecule}^{-1} \cdot \text{s}^{-1}$)		
		nitrogen	air	oxygen
hydrogen sulfide	propane	$(3.70 \pm 0.09) \times 10^{-12}$	$(4.08 \pm 0.10) \times 10^{-12}$	$(4.04 \pm 0.05) \times 10^{-12}$
dimethyl sulfide	propene	$(4.36 \pm 0.75) \times 10^{-12}$	$(8.67 \pm 0.28) \times 10^{-12}$	$(1.13 \pm 0.49) \times 10^{-11}$
ethyl methyl sulfide	propene	$(8.95 \pm 0.26) \times 10^{-12}$	$(1.46 \pm 0.36) \times 10^{-11}$	$(1.92 \pm 0.62) \times 10^{-11}$
thioethanol	propene	$(4.39 \pm 1.25) \times 10^{-11}$	$(3.89 \pm 0.57) \times 10^{-11}$	$(3.77 \pm 0.68) \times 10^{-11}$
<i>n</i> -butanethiol	propene	$(5.23 \pm 2.11) \times 10^{-11}$	$(4.16 \pm 0.99) \times 10^{-11}$	$(3.56 \pm 0.68) \times 10^{-11}$
<i>iso</i> -butanethiol	propene	$(4.65 \pm 1.34) \times 10^{-11}$	$(4.71 \pm 0.99) \times 10^{-11}$	$(3.74 \pm 0.42) \times 10^{-11}$

mental condition, and thus, the rate constants of $\cdot\text{OH}$ +thiols were corrected through the following expression:

$$\frac{(\text{dln}[\text{thiols}]/\text{dt})_{\alpha} - (\text{dln}[\text{thiols}]/\text{dt})_{\beta}}{(\text{dln}[\text{propene}]/\text{dt})_{\alpha} - (\text{dln}[\text{propene}]/\text{dt})_{\gamma}} = \frac{k_{\text{S}}}{k_{\text{R}}} \quad (4)$$

where $(\text{dln}[\text{thiols}]/\text{dt})_{\alpha}$ and $(\text{dln}[\text{propene}]/\text{dt})_{\alpha}$ are the first order decays of thiols and reference propene, respectively, obtained from analysis of thiol/propene/ $\text{H}_2\text{O}_2/\text{N}_2/\text{air}/\text{O}_2$ photolysis mixtures. $(\text{dln}[\text{thiols}]/\text{dt})_{\beta}$ is the first order decay of the thiol obtained from the analysis of thiols/ $\text{N}_2/\text{air}/\text{O}_2$ photolysis mixtures and represents the contribution due to photolysis. $(\text{dln}[\text{propene}]/\text{dt})_{\gamma}$ is the first order decay of propene obtained from the analysis of propene/thiols/ $\text{N}_2/\text{air}/\text{O}_2$ photolysis mixtures and represents the contribution because of the reaction $\text{HS}\cdot + \text{propene}$.

2 Results and discussion

All the experiments described below were conducted at room temperature (298.0 ± 1.5 K) and a total pressure of 1.01×10^5 Pa. The measured rate constants for each compound are given in Table 1. The errors quoted are twice the standard deviation arising from the least-squares fit of the straight lines and do not include an estimate of the error in the reference rate constants.

2.1 Reaction of $\cdot\text{OH}$ with H_2S

The rate constant for the reaction of $\cdot\text{OH}$ with H_2S , $\text{H}_2\text{S} + \cdot\text{OH} \rightarrow \text{HS}\cdot + \text{H}_2\text{O}$, was measured relative to that of $\cdot\text{OH}$ +propane (C_3H_8 , $k_{\text{propane}} = 1.09 \times 10^{-12} \text{ cm}^3 \cdot \text{molecule}^{-1} \cdot \text{s}^{-1}$ [19]). The initial concentrations of H_2S and C_3H_8 were in the range of $(20-50) \times 10^{13} \text{ molecule} \cdot \text{cm}^{-3}$. Typically, the reaction mixtures were irradiated for durations of 30 min to 3 h leading to a consumption of 20% to 90% of the initial concentration of the reactants at the start of irradiation. To test if the measured rate constant for the reaction of $\cdot\text{OH}$ with H_2S was O_2 -dependent, the experiments were carried out with nitrogen, air, and oxygen as bath gases, respectively.

Fig. 1 shows plots of $\ln\{[\text{H}_2\text{S}]_0/[\text{H}_2\text{S}]_t\}$ versus $\ln\{[\text{C}_3\text{H}_8]_0/[\text{C}_3\text{H}_8]_t\}$ for the reaction of $\text{H}_2\text{S} + \cdot\text{OH}$. The rate constant of $(4.08 \pm 0.10) \times 10^{-12} \text{ cm}^3 \cdot \text{molecule}^{-1} \cdot \text{s}^{-1}$ was obtained for the reaction between $\cdot\text{OH}$ and H_2S in air at 1.01×10^5 Pa and 298 K.

The rate constants for the reaction under different bath gases (air, N_2 , and O_2) were within the experimental error limits, indicating that the measured rate constants were independent of O_2 . The rate constants of the reactions at room temperature determined in this study were compared with the previously reported data[10-21] in Table 2.

The rate constants obtained by this study were in good agreement with the values measured by Cox and Sheppard[13] and

Barnes *et al.*[19], who also used a relative-rate technique. Apart from the highest value of $k = (5.5 \pm 0.3) \times 10^{-12} \text{ cm}^3 \cdot \text{molecule}^{-1} \cdot \text{s}^{-1}$ reported by Westenberg and de Haas[10] and the lowest value of $k = 2.62 \times 10^{-12} \text{ cm}^3 \cdot \text{molecule}^{-1} \cdot \text{s}^{-1}$ reported by Mousavipour *et al.*[21], the rate constants for the reactions under different buffer gases determined by other investigators using absolute techniques are also consistent with our results within the combined error limits.

2.2 Reactions of $\cdot\text{OH}$ with DMS and EMS

The rate constants for the reaction of $\cdot\text{OH}$ with DMS have been measured using the relative method in previous study[13]. However, the database for the reaction of $\cdot\text{OH}$ with EMS is still scarce. Fig. 2 shows plots of $\ln\{[\text{S}]_0/[\text{S}]_t\}$ versus $\ln\{[\text{R}]_0/[\text{R}]_t\}$ for reactions of $\text{DMS} + \cdot\text{OH}$ and $\text{EMS} + \cdot\text{OH}$.

The rate constant was derived from the least-squares analysis of such plots placed on an absolute basis using a rate constant for the reaction of $\cdot\text{OH}$ with propene of $k_{\text{propene}} = 2.6 \times 10^{-11} \text{ cm}^3 \cdot \text{molecule}^{-1} \cdot \text{s}^{-1}$ [19]. The average values derived from different experiments are shown in Table 1.

From Fig. 2, we can see that the rate constants of $\text{DMS} + \cdot\text{OH}$ and $\text{EMS} + \cdot\text{OH}$ increased with O_2 partial pressure. The obtained rate constant for the reaction of $\text{EMS} + \cdot\text{OH}$ in this study is in good agreement with the only one value reported by Hynes *et al.*[22], who used an absolute-rate technique. A number of investigations have been made for the reaction of $\text{DMS} + \cdot\text{OH}$ using both absolute and relative rate methods[23,24]. The detailed comparison of the rate constants determined in this and other studies was made by another article, and a good review was reported by Barnes *et al.*[25].

Two different channels for the reaction of $\cdot\text{OH} + \text{R}_1\text{—S—R}_2$ can be envisaged: direct abstraction path leading to the formation of

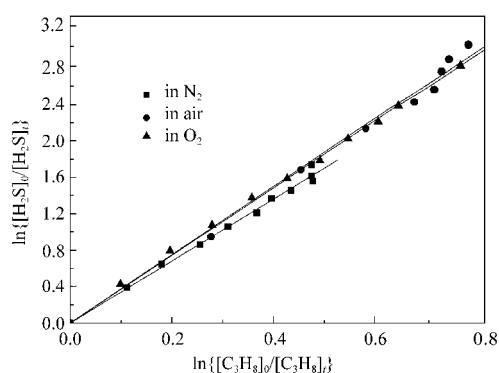


Fig. 1 Plots of $\ln\{[\text{H}_2\text{S}]_0/[\text{H}_2\text{S}]_t\}$ versus $\ln\{[\text{C}_3\text{H}_8]_0/[\text{C}_3\text{H}_8]_t\}$ in $\text{H}_2\text{O}_2/\text{N}_2/\text{air}/\text{O}_2$ mixtures at 1.01×10^5 Pa and 298 K

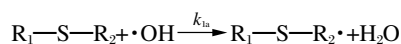
Table 2 Summary of present results and other measurements near 298 K of $\cdot\text{OH}+\text{H}_2\text{S}$ reaction

T/K	$10^{12}k/(\text{cm}^3\cdot\text{molecule}^{-1}\cdot\text{s}^{-1})$	p/Pa	Buffer gas	Technique	Reference
298	5.5 ± 0.3	199.5–292.6	He	FF-ESR	[10]
298	3.1 ± 0.5	2660	He	PP-RF	[11]
297.5	5.25 ± 0.53	3990–6650	Ar	FP-RF	[12]
297	5.0 ± 0.3	1.01×10^5	air	CP-GC	[13]
297	5.13 ± 0.57	5320	Ar	FP-RF	[14]
295	4.42 ± 0.48	6650–11970	Ar	FP-RF	[15]
298	3.9 ± 0.7		He	DF-RF	[16]
298	4.42 ± 0.36	2660–15960	Ar	FP-RF	[17]
299	4.38 ± 0.08	106.4–465.5	He	DF-RF	[18]
300	4.38 ± 0.03	146.3–465.5	N_2	DF-RF	[18]
300	4.34 ± 0.08	146.3–465.5	O_2	DF-RF	[18]
300	5.2 ± 0.8	1.01×10^5	air	CP-GC	[19]
294	3.3 ± 0.5	0–1330	He	DF-RF & DF-LIF	[20]
298	2.62			TS	[21]
298	3.70 ± 0.09	1.01×10^5	N_2	CP-GC	this work
298	4.08 ± 0.10	1.01×10^5	air	CP-GC	this work
298	4.04 ± 0.05	1.01×10^5	O_2	CP-GC	this work

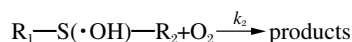
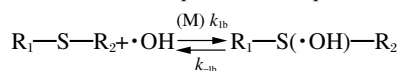
FF: fast flow, ESR: electron spin resonance, PP: pulsed photolysis, FP: flash photolysis, RF: resonance fluorescence, DF: discharge flow, TS: theory study,

LIF: laser induced fluorescence; CP: continuous photolysis, GC: gas chromatography

H_2O and $\text{R}_1-\text{S}-\text{R}_2\cdot$ in the absence of O_2



and reversible addition, of which the triplet collision complex formed, becomes important in the presence of O_2



where in the present work R represents CH_3 and/or C_2H_5 .

In this article, we only discuss the studies on the O_2 partial pressure and the third-body effect of these two S-contained compounds. Fig.3 shows the O_2 dependence of k for reactions $\cdot\text{OH}+\text{DMS}$ and $\cdot\text{OH}+\text{EMS}$ at room temperature, for comparison, the results of Refs. [21,22] are also shown. The experimental observations of DMS and EMS are consistent by following a simple kinetic analysis on the basis of an assumption of a steady state for $\text{R}_1-\text{S}(\cdot\text{OH})-\text{R}_2$:

$$k_{\text{eff}}=k_{\text{ia}}+\frac{k_{\text{ib}}[\text{O}_2]}{k_{-\text{ib}}/k_2+r} \quad (5)$$

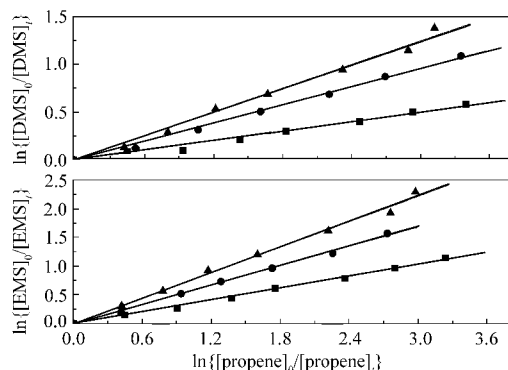


Fig.2 Plots of $\ln\{[S]_0/[S]_t\}$ versus $\ln\{[R]_0/[R]_t\}$ in $\text{H}_2\text{O}_2/\text{N}_2/\text{air}/\text{O}_2$ mixtures at 1.01×10^5 Pa and 298 K

● in air; ▲ in O_2 ; ■ in N_2

where k_{eff} is the measured effective second-order rate constant for the $\cdot\text{OH}+\text{R}_1-\text{S}-\text{R}_2$ (R_1 and $\text{R}_2\neq\text{H}$) reaction; r is the ratio of $p_{\text{O}_2}/p_{\text{M}}$. In the absence of O_2 , the reaction of $\cdot\text{OH}$ with $\text{R}_1-\text{S}-\text{R}_2$ (R_1 and $\text{R}_2\neq\text{H}$) is thought to proceed totally *via* the abstraction route (1a).

At 298 K, our results show a branching ratio value of 0.5 and 0.6 for the abstraction channel as DMS and EMS, respectively. Under atmospheric conditions, the addition channel is likely to be as important as the abstraction channel.

2.3 Reaction of $\cdot\text{OH}$ with aliphatic thiols

We also investigated the rate constant of the reaction between $\cdot\text{OH}$ radicals and RSH ($\text{R}\neq\text{H}$), $\text{RSH}+\cdot\text{OH}\rightarrow\text{RS}\cdot+\text{H}_2\text{O}$. As mentioned in experimental section, obvious losses of propene and thiols were observed during photolysis of the mixture of thiols and propene under different bath gases without H_2O_2 presence, however, on irradiation of propene in O_2 , air, and N_2 , respectively, without the thiols, no loss of propene was observed. These

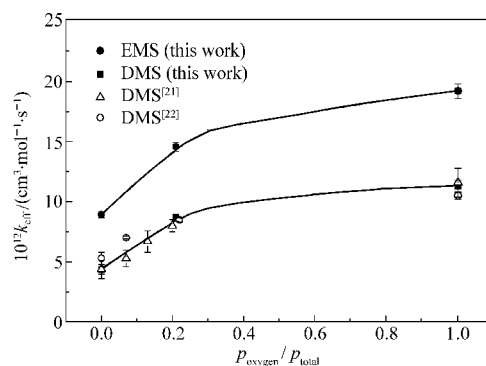


Fig.3 Comparison of the literature values with those of the relative rate constant study for the effective rate constants for $\cdot\text{OH}+\text{DMS}$ and $\cdot\text{OH}+\text{EMS}$ as a function of O_2 partial pressure at a total pressure of 1.01×10^5 Pa (N_2+O_2) and 298 K

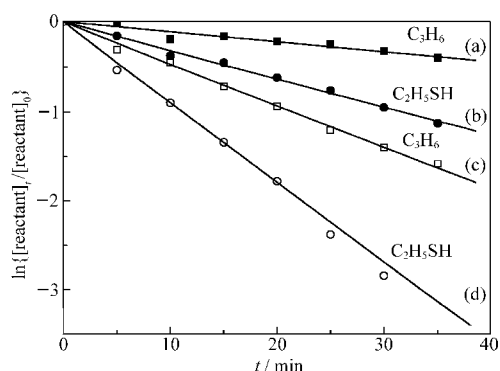


Fig.4 Typical $\ln\{[\text{reactant}]_t/[\text{reactant}]_0\}$ versus t plots for a $\text{C}_2\text{H}_5\text{SH}/\text{H}_2\text{O}_2/\text{propene}$ photolysis system at a total pressure of 1.01×10^5 Pa (N_2) and 298 K in a 300-L Teflon bag

Plots (a) and (b) are the decay of C_3H_6 and $\text{C}_2\text{H}_5\text{SH}$ in the absence of H_2O_2 , and plots (c) and (d) are the decay of C_3H_6 and $\text{C}_2\text{H}_5\text{SH}$ in the presence of H_2O_2 , respectively.

experimental phenomena indicated that the products from photolysis of the thiols could consume propene. Although there is no published work about the reaction between propene and the photolysis products of thiols, the following mechanism could be assumed for the reaction as the reaction of C_3H_6 with $\text{HS}\cdot$:

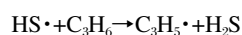
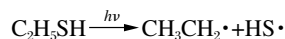


Fig.4 shows the typical decay curves for $\text{C}_2\text{H}_5\text{SH}$ (lines (b) and (d)) and propene (lines (a) and (c)). As shown in Fig.4, line (a) is the first order decay plot for propene because of the reaction with $\text{HS}\cdot$, and line (b) is the result from a $\text{C}_2\text{H}_5\text{SH}/\text{propene}/\text{H}_2\text{O}_2/\text{air}$ system. Line (c) is the first order decay plot for propene because of a combination of reaction with $\text{HS}\cdot$ and reaction with $\cdot\text{OH}$, and line (d) is the first order decay for $\text{C}_2\text{H}_5\text{SH}$ due to a combination of direct photolysis and reaction with $\cdot\text{OH}$. The experimental data for each substance when plotted with equation (4) gave good straight lines as shown in Fig.4 and Table 1, where the indicated errors represent two least squares standard deviation and no uncertainties in the rate constants of reference

Table 3 Summary of present results and other measurements near 298 K of $\cdot\text{OH} + \text{thiols}$ reaction

Sulfide	$10^{11}k/(\text{cm}^3 \cdot \text{molecule}^{-1} \cdot \text{s}^{-1})$	p/Pa	Buffer gas	Technique	Reference
$\text{C}_2\text{H}_5\text{SH}$	3.67 ± 0.18	2261–3325	Ar	DF-RF	[26]
	4.52 ± 0.36	3990	Ar	FP-RF	[27]
	2.7 ± 0.2	53.2–106.4	He	DF-ESR-mass	[28]
	4.5 ± 0.5	1.01×10^5	N_2	CP-GC	[19]
	4.39 ± 1.25	1.01×10^5	N_2	CP-GC	this work
	3.89 ± 0.57	1.01×10^5	air	CP-GC	this work
$n\text{-C}_4\text{H}_9\text{SH}$	3.77 ± 0.68	1.01×10^5	O_2	CP-GC	this work
	4.38 ± 0.66	9975	Ar	FP-RF	[27]
	5.6 ± 0.4	1.01×10^5	N_2	CP-GC	[19]
	5.23 ± 3.11	1.01×10^5	N_2	CP-GC	this work
	4.16 ± 0.99	1.01×10^5	air	CP-GC	this work
$iso\text{-C}_4\text{H}_9\text{SH}$	3.56 ± 0.68	1.01×10^5	O_2	CP-GC	this work
	4.18 ± 0.08	9975	Ar	FP-RF	[27]
	4.6 ± 0.5	1.01×10^5	N_2	CP-GC	[19]
	4.65 ± 1.37	1.01×10^5	N_2	CP-GC	this work
	4.71 ± 0.99	1.01×10^5	air	CP-GC	this work
	3.74 ± 0.42	1.01×10^5	O_2	CP-GC	this work

were considered. The rate constants for $\text{C}_2\text{H}_5\text{SH}$, $n\text{-C}_4\text{H}_9\text{SH}$, and $iso\text{-C}_4\text{H}_9\text{SH}$ in this study are compared with the values reported previously in the published work^[19,26–28] in Table 3. The agreement between this work and published data is generally good. The only exception is the very low value obtained by MacLeod *et al.*^[28] for $\cdot\text{OH} + \text{C}_2\text{H}_5\text{SH}$ in He using DF-ESR-mass by absolute method.

The trend in the rates of $\cdot\text{OH} + \text{thiols}$ reaction in N_2 , air, and O_2 is not similar to that of the corresponding photochemical reactions of $\cdot\text{OH}$ with DMS and EMS. There are three possible pathways for the reaction of $\cdot\text{OH}$ with the aliphatic thiols: (i) abstraction of a H atom from the C—H bonds, (ii) abstraction of a H atom from S—H bond, and (iii) addition of $\cdot\text{OH}$ to S atom. In this work, the rate constants for the three aliphatic thiols determined in N_2 (1.01×10^5 Pa) at 298 K lie in the range of 4.39×10^{-11} to $5.43 \times 10^{-11} \text{ cm}^3 \cdot \text{molecule}^{-1} \cdot \text{s}^{-1}$, and agree well with published work. Although the rate constants increase in a manner expected with the various combinations of primary, secondary, and tertiary C—H bonds, the increase is small compared to that which would be expected if H abstraction from the C atom was a major pathway. This indicates that H abstraction from the C atom is a minor channel as has already been suggested by Wine^[27] and Barnes^[19] *et al.* from their studies on the same thiols. They have also concluded that abstraction of a H atom from the sulfide is also a minor channel since they failed to detect an isotope effect between the reactions of $\cdot\text{OH}$ with CH_3SH and CH_3SD which would have been expected if a H atom abstraction from sulfide was an important reaction pathway.

2.4 Structure–activity relationships (SARs)

The rate constants reported for the reduced sulfur compounds can be compared to the rate constants calculated from the one developed by Atkinson^[29,30].

In this relationship, the calculation of H-atom abstraction rate constants from C—H bonds is based upon the estimation of $-\text{CH}_3$, $-\text{CH}_2-$, and $>\text{CH}-$ group rate constants. These depend on the nature of the substituents around these groups, with

$$k(\text{CH}_3\text{—X})=k_{\text{prim}}^0 F(\text{X})$$

$$k(\text{X—CH}_2\text{—Y})=k_{\text{sec}}^0 F(\text{X})F(\text{Y})$$

$$k[\text{X—CH}(\text{Y})\text{—Z}]=k_{\text{tert}}^0 F(\text{X})F(\text{Y})F(\text{Z})$$

where k_{prim}^0 , k_{sec}^0 , and k_{tert}^0 are the rate constants per —CH_3 , $\text{—CH}_2\text{—}$, and >CH— group for a standard substituent (—CH_3 , with $F(\text{—CH}_3)=1.00$); X, Y, and Z are the substituent groups, and $F(\text{X})$, $F(\text{Y})$, and $F(\text{Z})$ are the corresponding substituent factors. At room temperature, the values of k_{prim}^0 , k_{sec}^0 , and k_{tert}^0 (in the unit of $10^{-12} \text{ cm}^3 \cdot \text{molecule}^{-1} \cdot \text{s}^{-1}$) are 0.144, 0.838, and 1.83, and the factors of both $F(\text{—CH}_2\text{—})$ and $F(\text{>CH—})$ are 1.29. The data for the $\text{R}_1\text{—S—R}_2$ yield the factors $F(\text{—SH})=F(\text{—S—})=9.0$, and the group rate constants $k_{\text{—SH}}=3.1 \times 10^{-11} \text{ cm}^3 \cdot \text{molecule}^{-1} \cdot \text{s}^{-1}$ and $k_{\text{—S—}}=2.0 \times 10^{-12} \text{ cm}^3 \cdot \text{molecule}^{-1} \cdot \text{s}^{-1}$.

Using these group rate constants and substituent factors, and assuming that $\cdot\text{OH}$ interaction only occurs with the abstraction of H atom from the C—H bonds, then rate constants at 298 K for the reactions of $\cdot\text{OH}$ with CH_3SCH_3 , $\text{C}_2\text{H}_5\text{SCH}_3$, $\text{C}_2\text{H}_5\text{SH}$, $\text{CH}_3\text{CH}_2\text{CH}_2\text{CH}_2\text{SH}$, and $(\text{CH}_3)_2\text{CHCH}_2\text{SH}$ of 4.59×10^{-12} , 11.02×10^{-12} , 3.87×10^{-12} , 4.20×10^{-12} , and $4.20 \times 10^{-12} \text{ cm}^3 \cdot \text{molecule}^{-1} \cdot \text{s}^{-1}$, respectively, can be calculated. The excellent agreement of the calculated and experimental room temperature rate constants for these reduced sulfide compounds indicates that the structure–reactivity relationship can be used with confidence to calculate the rate constants for the reaction of $\cdot\text{OH}$ with this general class of reduced sulfide compounds.

3 Conclusions

We have described measurements of the reactions of $\cdot\text{OH}$ with H_2S , DMS, EMS, $\text{C}_2\text{H}_5\text{SH}$, $n\text{-C}_4\text{H}_9\text{SH}$, and $iso\text{-C}_4\text{H}_9\text{SH}$, with particular emphasis on the influence of O_2 partial pressure. We have performed $\cdot\text{OH}$ relative rate studies with DMS and EMS to investigate the influence of O_2 concentration by varying buffer gases. At 298 K, reactions of $\cdot\text{OH}$ with DMS and EMS were observed to be increased with increasing partial pressure of O_2 . The results, together with the positive Arrhenius activation energies, indicated that H-atom abstraction and $\cdot\text{OH}$ addition were two independent reaction pathways. For DMS and EMS, two possible reaction pathways have been considered: adduct formation by the addition of $\cdot\text{OH}$. However, our results showed that not all the $\text{R}_1\text{—S—R}_2$ had observable O_2 partial pressure enhancement of the total rate. These data compared with previous $\cdot\text{OH}$ reactivity studies towards $\text{R}_1\text{—S—R}_2$ suggested that there might be a deactivation effect of H_2S , $n\text{-C}_4\text{H}_9\text{SH}$, and $iso\text{-C}_4\text{H}_9\text{SH}$ and positive effect of DMS, EMS, and $\text{C}_2\text{H}_5\text{SH}$ in the presence of O_2 .

Our results confirmed that $\cdot\text{OH}$ reacted rapidly with $\text{R}_1\text{—S—R}_2$, which was of atmospheric importance. We can obtain maximum tropospheric residence times, from the following relationship: $\tau^{-1} = k[\cdot\text{OH}]$, where $[\cdot\text{OH}]$ is an average value over the appropriate time interval. $\cdot\text{OH}$ levels are highly variable, depending on the local concentrations of O_3 , H_2O , CO , CH_4 , and NO_x , and also the solar UV flux. Using the $\cdot\text{OH}$ reaction rate constants determined in this work and a $\cdot\text{OH}$ concentration of 2×10^6

cm^{-3} ^[31], we obtained the following lifetimes at 298 K: $\tau_{\text{H}_2\text{S}}=28 \text{ h}$, $\tau_{\text{CH}_3\text{SCH}_3}=16 \text{ h}$, $\tau_{\text{C}_2\text{H}_5\text{SCH}_3}=9.5 \text{ h}$, $\tau_{\text{C}_2\text{H}_5\text{SH}}=3.6 \text{ h}$, $\tau_{n\text{-C}_4\text{H}_9\text{SH}}=3.4 \text{ h}$, $\tau_{iso\text{-C}_4\text{H}_9\text{SH}}=2.9 \text{ h}$. Midday $\cdot\text{OH}$ levels are a factor of ca 3 larger than the diurnally average value, so the residence times of the short-lived species $\text{C}_2\text{H}_5\text{SH}$, $n\text{-C}_4\text{H}_9\text{SH}$, and $iso\text{-C}_4\text{H}_9\text{SH}$ will be a factor of 3 shorter at noon than the diurnally estimates suggest.

References

- Vila-Costa, M.; Simó, R.; Harada, H.; Gasol, J. M.; Slezak, D.; Kiene, R. P. *Science*, **2006**, *314*: 652
- Bates, T. S.; Cline, J. D.; Gammon, R. H.; Kelly-Hansen, S. R. *J. Geophys. Res.*, **1987**, *92*: 2930
- Watts, S. F. *Atmos. Environ.*, **2000**, *34*: 761
- Charlson, R. J.; Lovelock, J. E.; Andreae, M. O.; Warren, S. G. *Nature*, **1987**, *326*: 655
- Du, L.; Xu, Y. F.; Ge, M. F.; Jia, L.; Yao, L.; Wang, W. G. *Chem. Phys. Lett.*, **2007**, *436*: 36
- Du, L.; Xu, Y. F.; Ge, M. F.; Jia, L. *Atmos. Environ.*, **2007**, *41*: 7434
- Cox, R. A. *Chem. Rev.*, **2003**, *103*: 4533
- Wu, H.; Mu, Y. J.; Zhang, X. S.; Jiang, G. B. *Int. J. Chem. Kinet.*, **2003**, *35*: 81
- Atkinson, R. *Atmos. Chem. Phys.*, **2003**, *3*: 2233
- Westenberg, A. A.; de Haas, N. J. *Chem. Phys.*, **1973**, *59*: 6685
- Stuhl, F. *Ber. Bunsenges. Phys. Chem.*, **1974**, *78*: 230
- Perry, R. A.; Atkinson, R.; Pitts, J. N. J. *J. Chem. Phys.*, **1976**, *64*: 3237
- Cox, R. A.; Sheppard, D. *Nature*, **1980**, *284*: 330
- Wine, P. H.; Kreutter, N. M.; Gump, C. A.; Ravlshankara, A. R. *J. Phys. Chem.*, **1981**, *85*: 2660
- Lin, C. L. *Int. J. Chem. Kinet.*, **1982**, *14*: 593
- Leu, M. T.; Smith, R. H. *J. Phys. Chem.*, **1982**, *86*: 73
- Michael, J. V.; Nava, D. F.; Brobst, W. D.; Borkowski, R. P.; Stief, L. J. *J. Phys. Chem.*, **1982**, *86*: 81
- Lin, Y. L.; Wang, N. S.; Lee, Y. P. *Int. J. Chem. Kinet.*, **1985**, *17*: 1201
- Barnes, I.; Bastian, V.; Becker, K. H.; Fink, E. H.; Nelsen, W. *J. Atmos. Chem.*, **1986**, *4*: 445
- Lafage, C.; Pauwels, J. F.; Carlier, M.; Devolder, P. *J. Chem. Soc. Faraday Trans. 2*, **1987**, *83*: 731
- Mousavipour, S. H.; Namdar-Ghanbari, M. A.; Sadeghian, L. *J. Phys. Chem. A*, **2003**, *107*: 3752
- Hynes, A. J.; Wine, P. H.; Semmes, D. H. *J. Phys. Chem.*, **1986**, *90*: 4148
- Barnes, I.; Bastian, V.; Becker, K. H. *Int. J. Chem. Kinet.*, **1988**, *20*: 415
- Wallington, J.; Atkinson, R.; Tuazon, E. C.; Aschmann, S. M. *Int. J. Chem. Kinet.*, **1986**, *18*: 837
- Barnes, I.; Hjorth, J.; Mihalopoulos, N. *Chem. Rev.*, **2006**, *106*: 940
- Lee, J. H.; Tang, I. N. *J. Chem. Phys.*, **1983**, *78*: 6646
- Wine, P. H.; Thompson, R. J.; Semmes, D. H. *Int. J. Chem. Kinet.*, **1984**, *16*: 1623
- MacLeod, H.; Jourdain, J. L.; Poulet, G.; LeBras, G. *Atmos. Environ.*, **1984**, *18*: 2621
- Atkinson, R. *Int. J. Chem. Kinet.*, **1987**, *19*: 799
- Atkinson, R. *Environ. Toxicol. Chem.*, **1988**, *7*: 435
- Hein, R.; Crutzen, P.; Heimann-Fenter, M. *Global Biogeochem. Cycles*, **1997**, *91*: 43